

*Supporting information*

**Construction of bimetallic oxy-hydroxides based on Ni(OH)<sub>2</sub> nanosheets for sensitive non-enzymatic glucose detection via electrochemical oxidation and incorporation**

*Weiji Dai,\*<sup>1</sup> Bing Wu,<sup>1</sup> Fan Zhang,<sup>1</sup> Yuxi Huang,<sup>1</sup> Cuijiao Zhao,<sup>1</sup> Yudong Zhang,<sup>1</sup> Can Cui,<sup>1</sup> Jing Guo,<sup>2</sup> Saifang Huang\*<sup>1</sup>*

<sup>1</sup> School of Materials Science and Engineering, Jiangsu University of Science and Technology, Zhenjiang 212003, China

<sup>2</sup> School of Resources and Materials, Northeastern University at Qinhuangdao, Qinhuangdao 066004, China

\*Corresponding authors.

E-mail: daiweiji@just.edu.cn (W. Dai), s.huang@just.edu.cn (S. Huang)

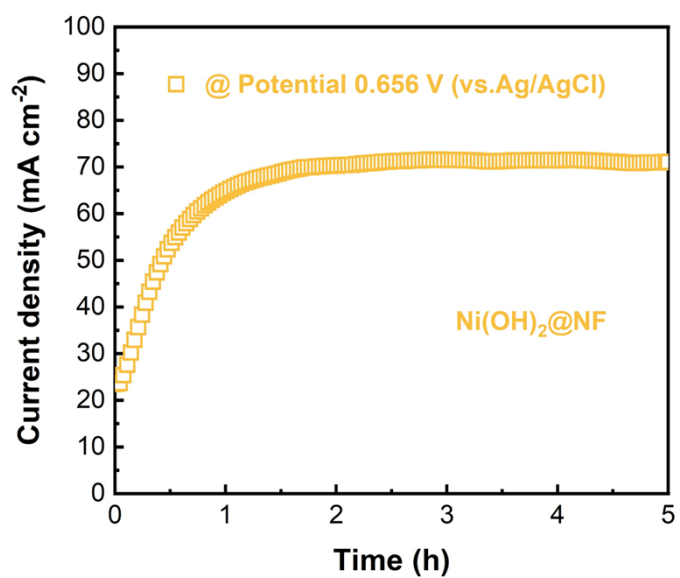


**Figure S1.** i-t curve of Ni(OH)<sub>2</sub>@NF at the potential of 0.656 V (vs. Ag/AgCl) in 1 M KOH solution.

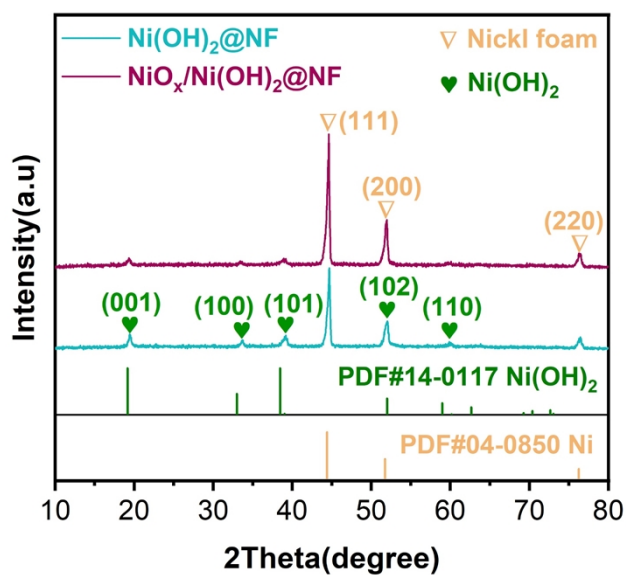


**Figure S2.** XRD pattern of Ni(OH)<sub>2</sub>@NF and NiO<sub>x</sub>/Ni(OH)<sub>2</sub>@NF.

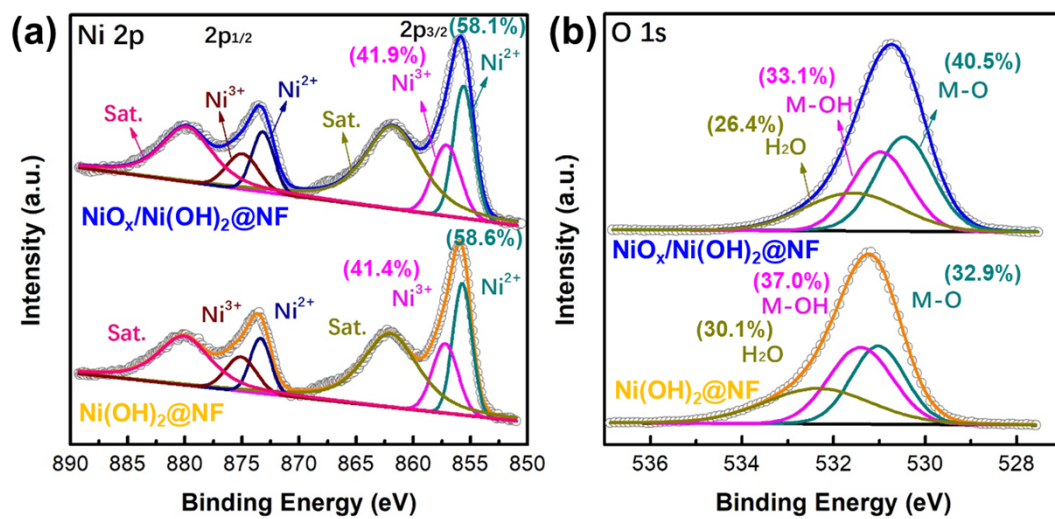


**Figure S3.** High-resolution XPS spectra: (a) Ni 2p, (b) O 1s.

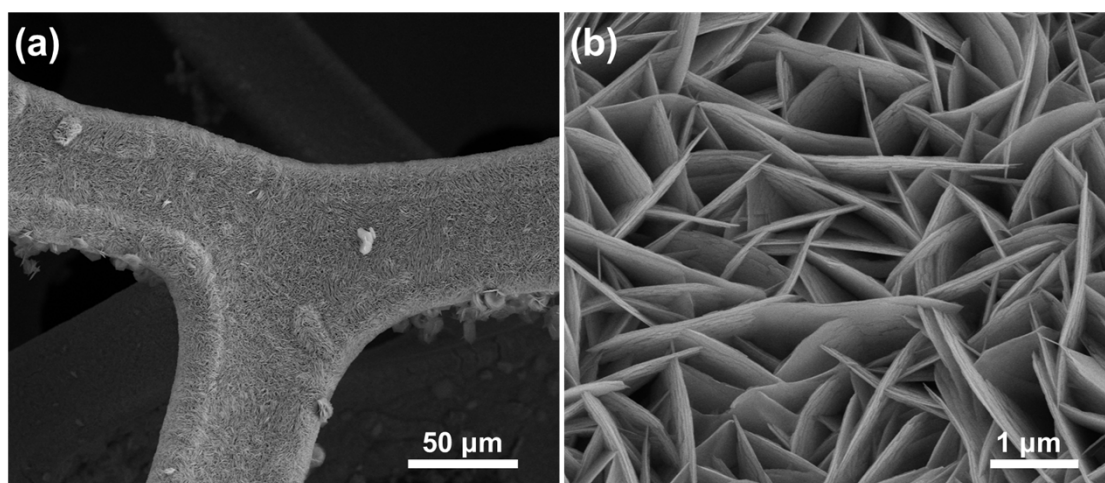


**Figure S4.** (a and b) SEM images of  $\text{Ni(OH)}_2@\text{NF}$ .

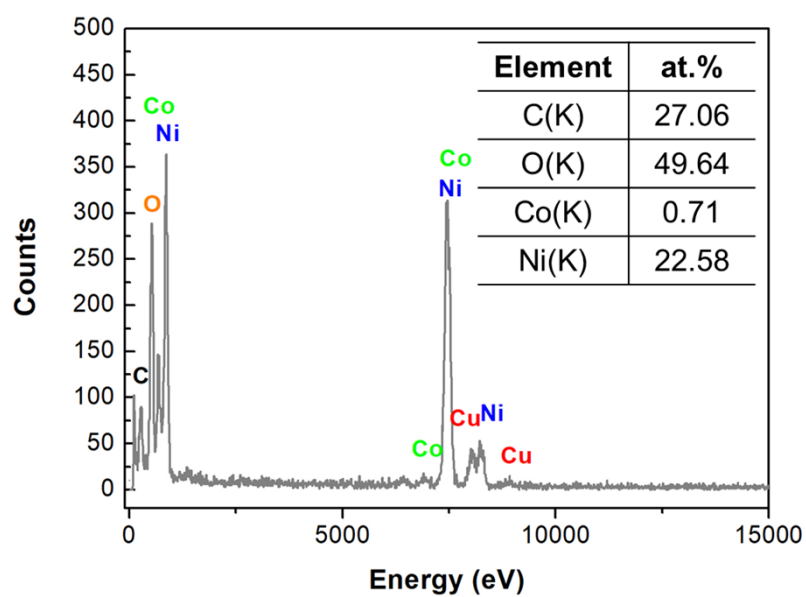


**Figure S5.** EDS pattern of  $(\text{CoNi})\text{O}_x/\text{Ni(OH)}_2@\text{NF}$ .

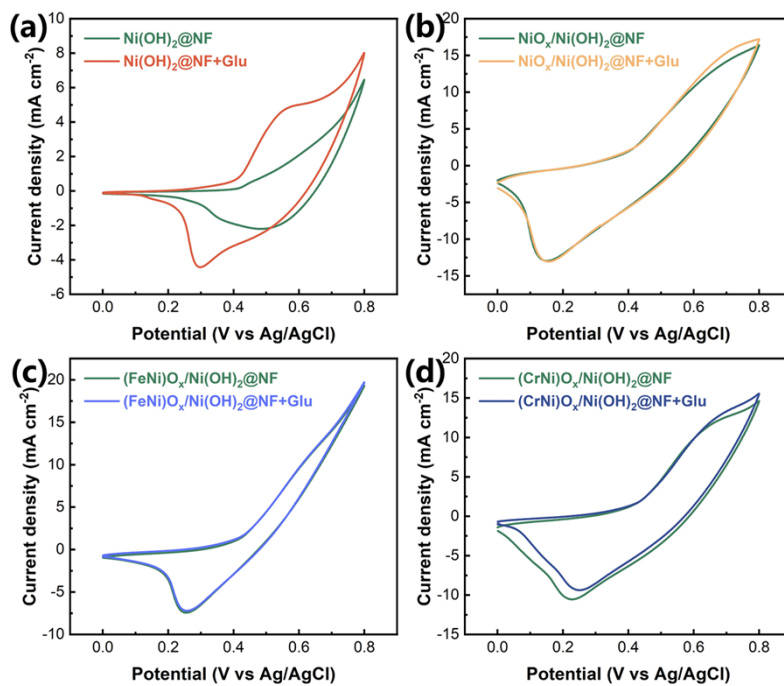


**Figure S6.** CV curves at scan rate of  $10 \text{ mV s}^{-1}$  with and without addition of  $1 \text{ mM}$  glucose: (a)  $\text{Ni(OH)}_2@\text{NF}$ , (b)  $\text{NiO}_x/\text{Ni(OH)}_2@\text{NF}$ , (c)  $(\text{FeNi})\text{O}_x/\text{Ni(OH)}_2@\text{NF}$ , and (d)  $(\text{CrNi})\text{O}_x/\text{Ni(OH)}_2@\text{NF}$ .

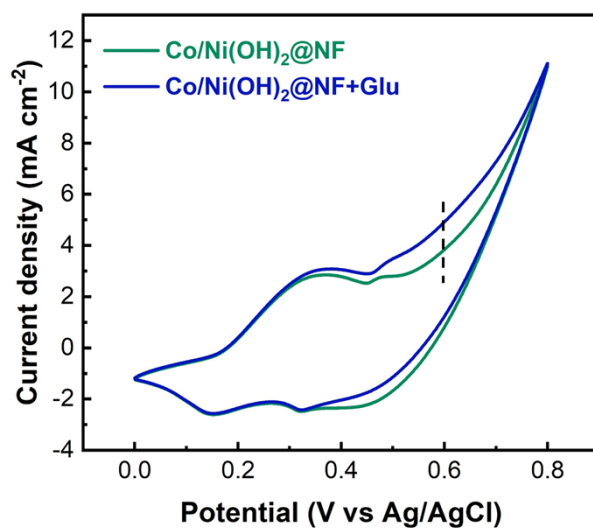


**Figure S7.** CV curves at scan rate of  $10 \text{ mV s}^{-1}$  with and without addition of  $1 \text{ mM}$  glucose.

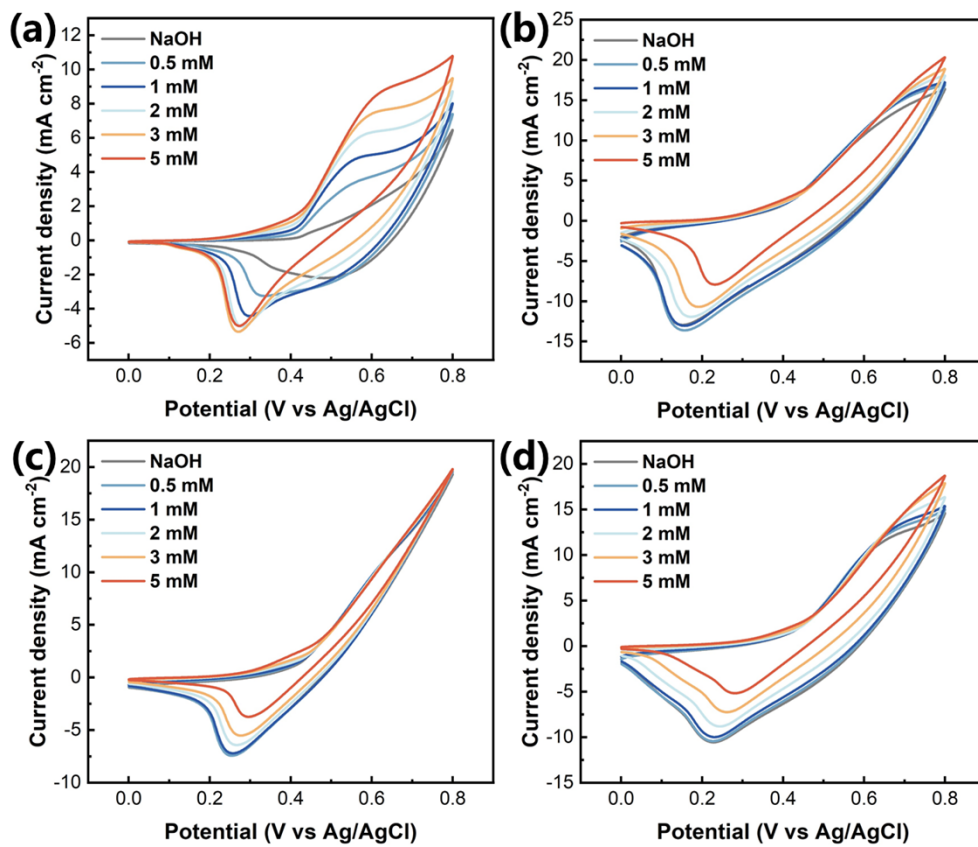


**Figure S8.** CV curves with addition of different concentration of glucose at scan rate of 10 mV s<sup>-1</sup>: (a) Ni(OH)<sub>2</sub>@NF, (b) NiO<sub>x</sub>/Ni(OH)<sub>2</sub>@NF, (c) (FeNi)O<sub>x</sub>/Ni(OH)<sub>2</sub>@NF, and (d) (CrNi)O<sub>x</sub>/Ni(OH)<sub>2</sub>@NF.

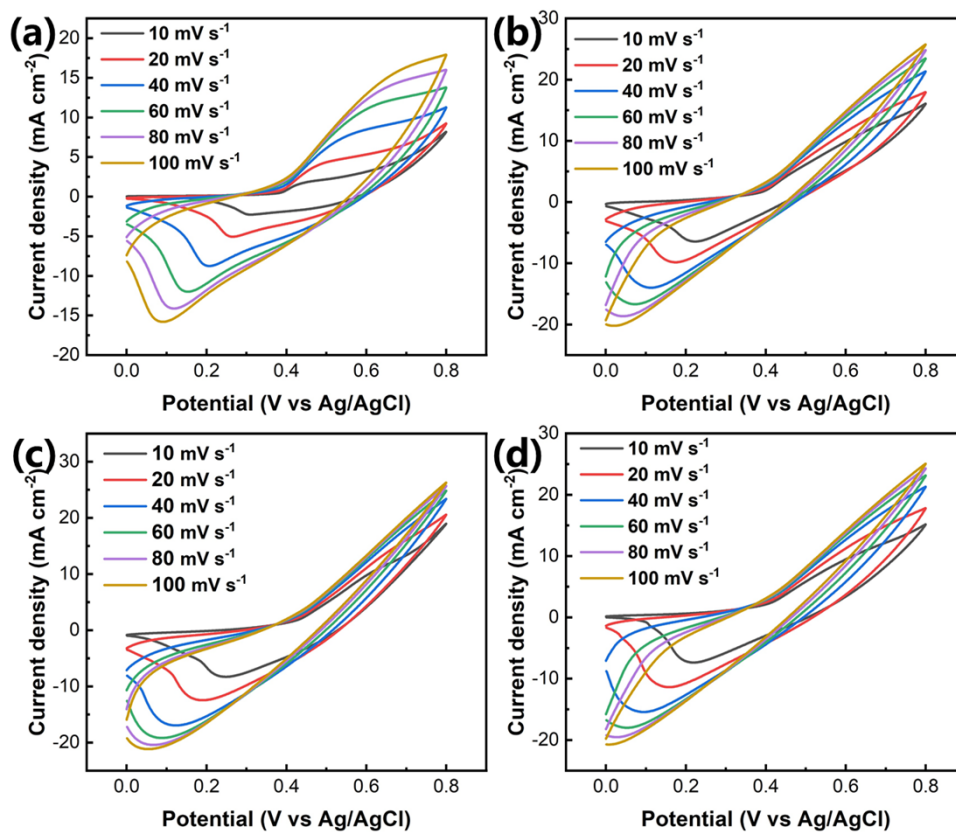


**Figure S9.** CV curves in a solution containing 0.1 M NaOH and 1 mM glucose with different scan rates ranging from 10 to 100 mV s<sup>-1</sup>: (a) Ni(OH)<sub>2</sub>@NF, (b) NiO<sub>x</sub>/Ni(OH)<sub>2</sub>@NF, (c) (FeNi)O<sub>x</sub>/Ni(OH)<sub>2</sub>@NF, and (d) (CrNi)O<sub>x</sub>/Ni(OH)<sub>2</sub>@NF.

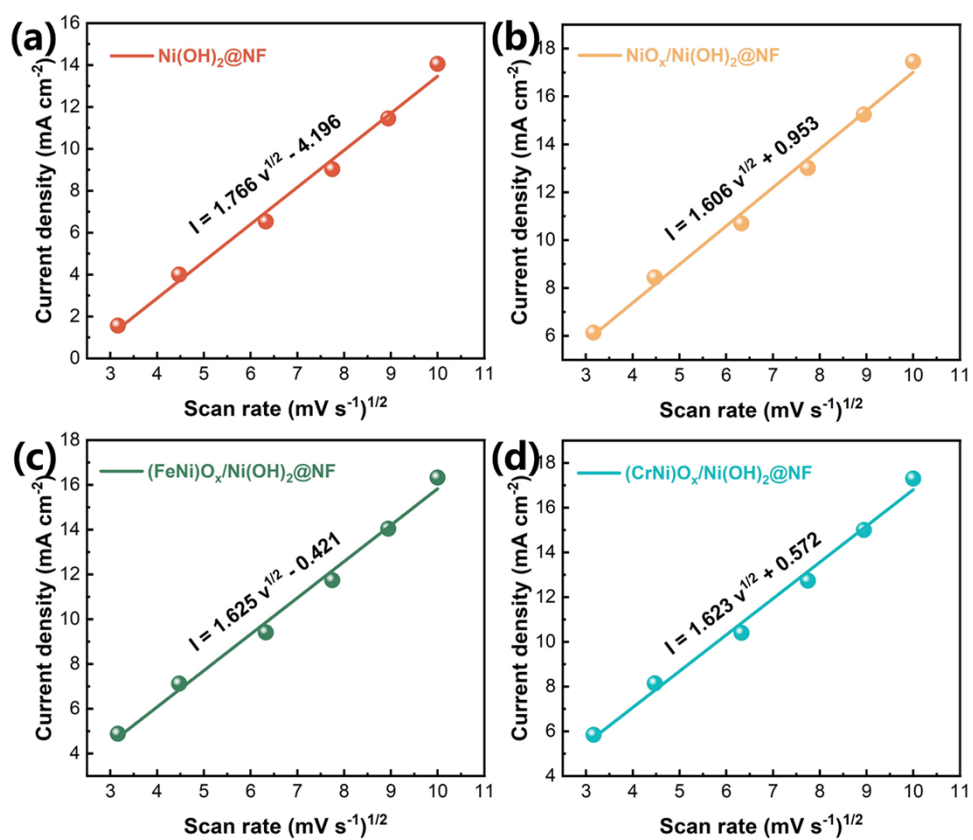


**Figure S10.** The current response versus the square root of the scan rate derived from the CV curves in Figure S8: (a)  $\text{Ni(OH)}_2@\text{NF}$ , (b)  $\text{NiO}_x/\text{Ni(OH)}_2@\text{NF}$ , (c)  $(\text{FeNi})\text{O}_x/\text{Ni(OH)}_2@\text{NF}$ , and (d)  $(\text{CrNi})\text{O}_x/\text{Ni(OH)}_2@\text{NF}$ .



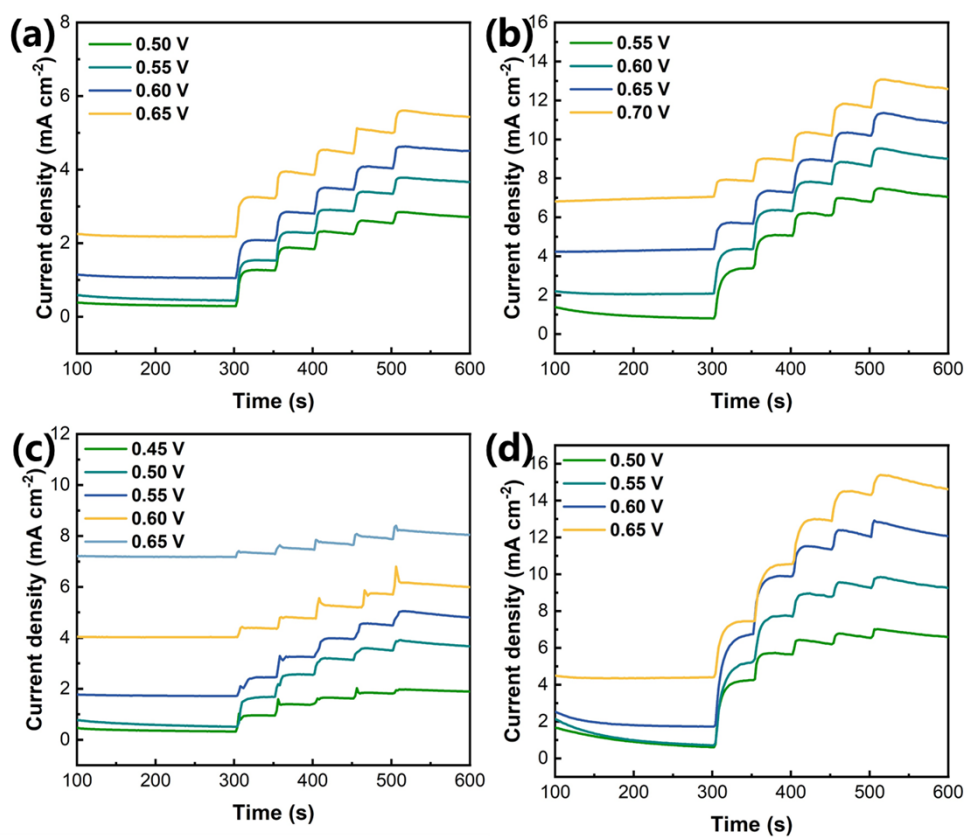


**Figure S11.** i-t curves at different voltages with incremental addition of 1 mM glucose:

(a) Ni(OH)<sub>2</sub>@NF, (b) NiO<sub>x</sub>/Ni(OH)<sub>2</sub>@NF, (c) (FeNi)O<sub>x</sub>/Ni(OH)<sub>2</sub>@NF, and (d) (CrNi)O<sub>x</sub>/Ni(OH)<sub>2</sub>@NF.

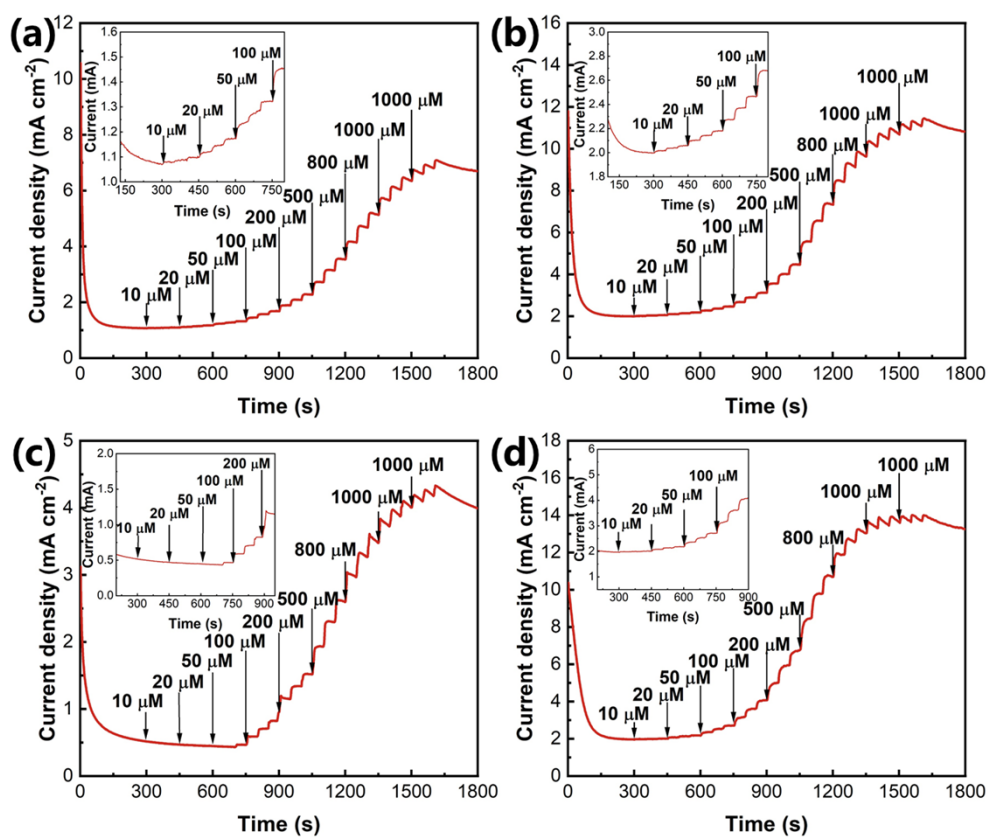


**Figure S12.** *i-t* curves with addition of different concentration of glucose: (a) Ni(OH)<sub>2</sub>@NF, (b) NiO<sub>x</sub>/Ni(OH)<sub>2</sub>@NF, (c) (FeNi)O<sub>x</sub>/Ni(OH)<sub>2</sub>@NF, and (d) (CrNi)O<sub>x</sub>/Ni(OH)<sub>2</sub>@NF.

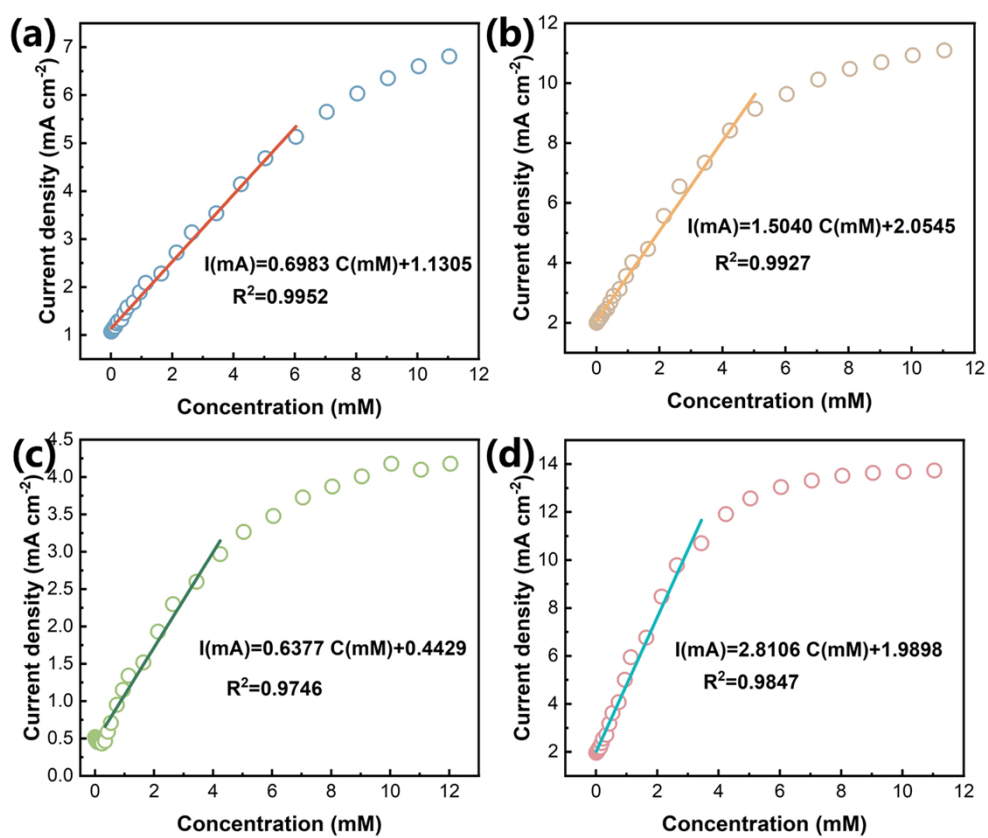


**Figure S13.** The corresponding concentration-current fitting curves derived from Figure S11: (a) Ni(OH)<sub>2</sub>@NF, (b) NiO<sub>x</sub>/Ni(OH)<sub>2</sub>@NF, (c) (FeNi)O<sub>x</sub>/Ni(OH)<sub>2</sub>@NF, and (d) (CrNi)O<sub>x</sub>/Ni(OH)<sub>2</sub>@NF.

**Table S1.** Sensing performances of electrocatalysts in recent literatures.

Electrocatalysts	Sensitivity	Linear range	References
	/mA mM <sup>-1</sup> cm <sup>-2</sup>	/mM	
Pt/Au/BDD	1.7	0.01-7.5	Biosensors and Bioelectronics 98 (2017) 76-82
NiCoFe-LDH/FF	5.717	0.01-0.1	Dalton Trans., 2023, 52, 16661- 16669
Hollow Ni(OH) <sub>2</sub> @CuS	2.74	0.01-6.64	Applied Surface Science 634 (2023) 157650
NiCo-LDH@NI-NTNW	3.4	~1.05	Journal of Colloid and Interface Science 591 (2021) 384-395
	4.6	1.05-2.52	Sensors & Actuators: B. Chemical 398 (2024) 134713
MOF-derived CuO/CNT	4.34	0.0005-0.1	Journal of The Electrochemical Society, 166 (16) B1732-B1741 (2019)
Ni(OH) <sub>2</sub> &NiOOH film/Ni	5.7584	0.001-0.13	Colloids and Surfaces A: Physicochemical and Engineering Aspects 703 (2024) 135301
			Electrochimica Acta 299 (2019) 470-478
CuO nanowire array	1.95	0.1-6	
<b>(CoNi)O<sub>x</sub>/Ni(OH)<sub>2</sub>@NF</b>	<b>3.59</b>	<b>0.01-1.14</b>	<b>This work</b>

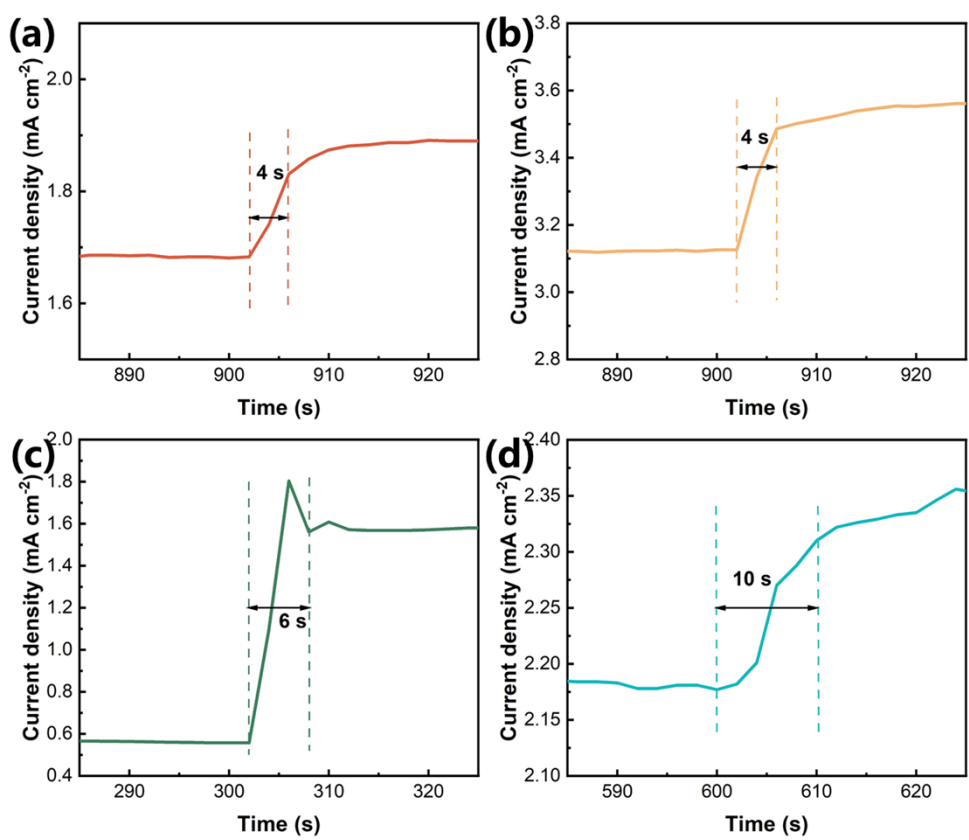


**Figure S14.** i-t curves with addition of 10 μM of glucose: (a) Ni(OH)<sub>2</sub>@NF, (b) NiO<sub>x</sub>/Ni(OH)<sub>2</sub>@NF, (c) (FeNi)O<sub>x</sub>/Ni(OH)<sub>2</sub>@NF, and (d) (CrNi)O<sub>x</sub>/Ni(OH)<sub>2</sub>@NF.

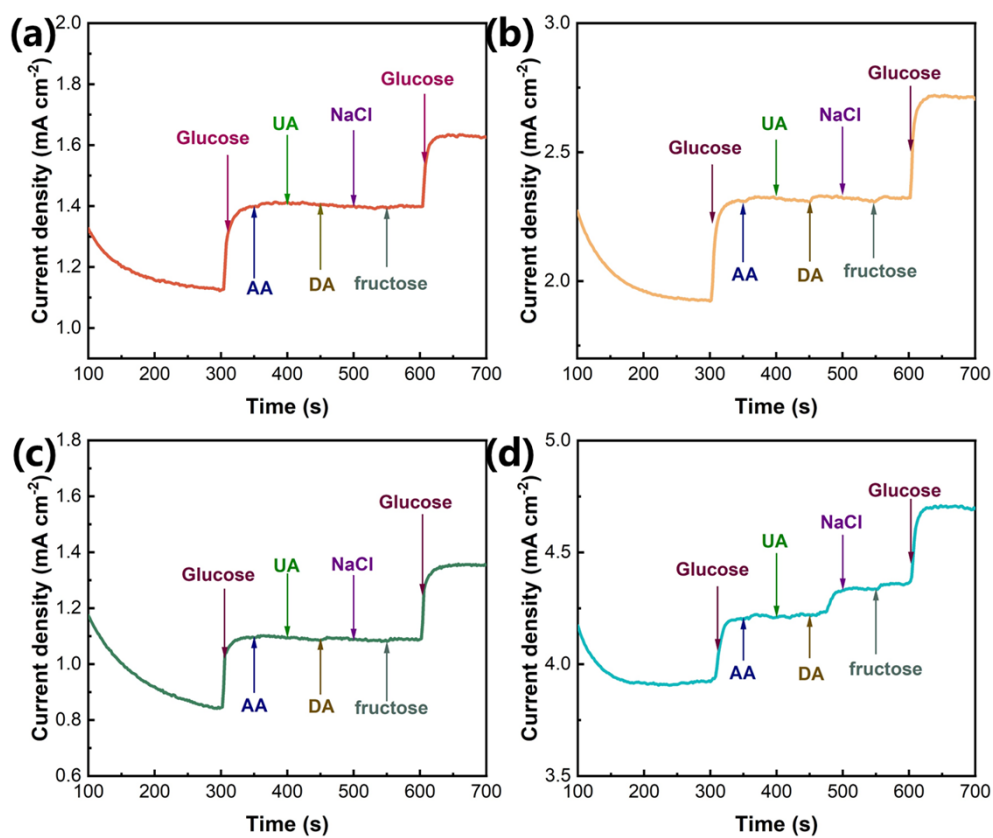


**Figure S15.** i-t curves with addition of with addition of glucose, AA, UA, DA, NaCl, and fructose: (a) Ni(OH)<sub>2</sub>@NF, (b) NiO<sub>x</sub>/Ni(OH)<sub>2</sub>@NF, (c) (FeNi)O<sub>x</sub>/Ni(OH)<sub>2</sub>@NF, and (d) (CrNi)O<sub>x</sub>/Ni(OH)<sub>2</sub>@NF.

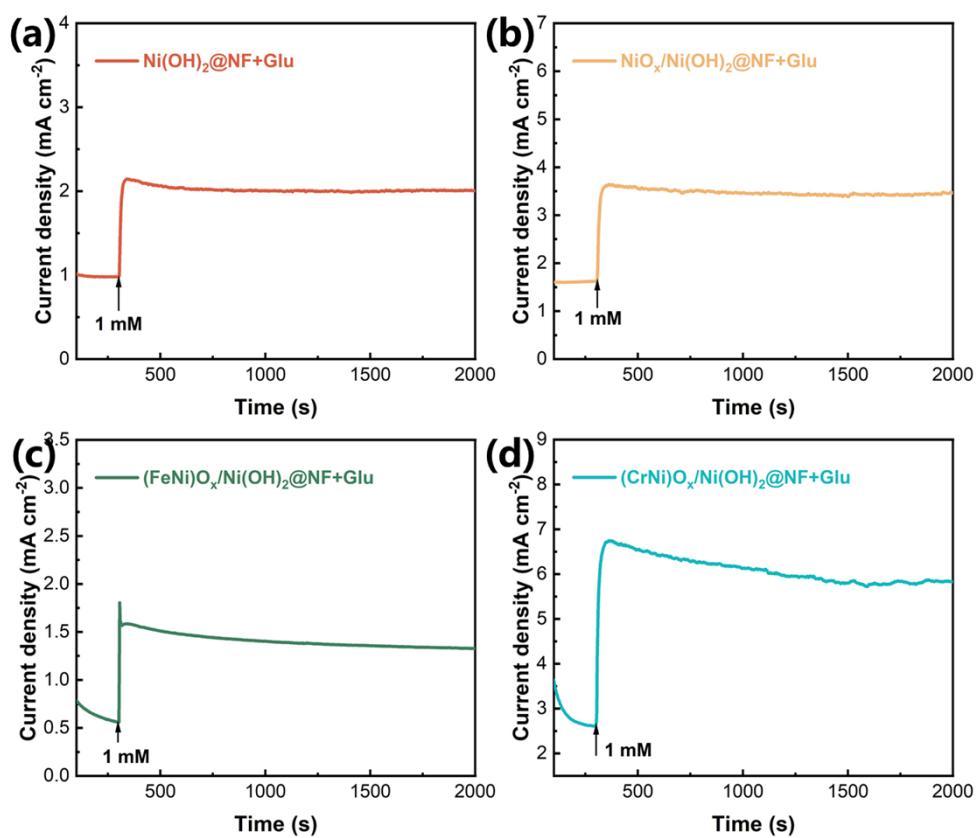


**Figure S16.** Long-term stability tests with addition of 1 mM glucose: (a)  $\text{Ni(OH)}_2@\text{NF}$ , (b)  $\text{NiO}_x/\text{Ni(OH)}_2@\text{NF}$ , (c)  $(\text{FeNi})\text{O}_x/\text{Ni(OH)}_2@\text{NF}$ , and (d)  $(\text{CrNi})\text{O}_x/\text{Ni(OH)}_2@\text{NF}$ .